J|A|C|S
ARTICLES
Published on Web 08/08/2006

Solid-State ^{2}H NMR Structure of Retinal in Metarhodopsin I

Gilmar F. J. Salgado,[†,⊥] Andrey V. Struts,[‡] Katsunori Tanaka,[||,#] Sonja Krane,[||,¶] Koji Nakanishi,[||] and Michael F. Brown*[,†,‡,§]

Contribution from the Department of Biochemistry & Molecular Biophysics, Department of Chemistry, and Department of Physics, University of Arizona, Tucson, Arizona 85721, and Department of Chemistry, Columbia University, New York, New York 10027

Received December 23, 2005; Revised Manuscript Received March 23, 2006; E-mail: mfbrown@u.arizona.edu

Abstract: The structural and photochemical changes in rhodopsin due to absorption of light are crucial for understanding the process of visual signaling. We investigated the structure of *trans*-retinal in the metarhodopsin I photointermediate (MI), where the retinylidene cofactor functions as an antagonist. Rhodopsin was regenerated using retinal that was ^{2}H-labeled at the C5, C9, or C13 methyl groups and was reconstituted with 1-palmitoyl-2-oleoyl-*sn*-glycero-3-phosphocholine. Membranes were aligned by isopotential centrifugation, and rhodopsin in the supported bilayers was then bleached and cryotrapped in the MI state. Solid-state ^{2}H NMR spectra of oriented rhodopsin in the low-temperature lipid gel state were analyzed in terms of a static uniaxial distribution (Nevzorov, A. A.; Moltke, S.; Heyn, M. P.; Brown, M. F. *J. Am. Chem. Soc.* **1999**, *121*, 7636−7643). The line shape analysis allowed us to obtain the methyl bond orientations relative to the membrane normal in the presence of substantial alignment disorder (mosaic spread). Relative orientations of the methyl groups were used to calculate effective torsional angles between the three different planes that represent the polyene chain and the β-ionone ring of retinal. Assuming a three-plane model, a less distorted structure was found for retinal in MI compared to the dark state. Our results are pertinent to how photonic energy is channeled within the protein to allow the strained retinal conformation to relax, thereby forming the activated state of the receptor.

Introduction

G protein coupled receptors (GPCRs) are involved in the recognition and signal transduction of intracellular messages.[1] They constitute the largest gene family in the human genome and are the targets of ≈50% of all pharmaceuticals. Rhodopsin is a prototypical family A GPCR and is responsible for scotopic (dim light) vision. Moreover, opsin class receptors are implicated in diverse physiological processes as photic regulators involving circadian clocks, pupillary constriction, and skin pigmentation.[2] So far, rhodopsin (Rho) is the only GPCR for which a high-resolution three-dimensional crystal structure is available.[3] Absorption of a photon by Rho gives 11-*cis* to *trans* isomerization of the retinylidene ligand, followed by conformational changes that trigger interactions with effector proteins, leading to visual perception.[4] Distortion of retinal[5−7] is linked to its ultrafast photochemistry,[8] yet high-resolution structural knowledge is lacking of the photointermediates of Rho upon illumination. Here we applied solid-state ^{2}H NMR (reviewed in ref 9) to acquire orientational restraints for *trans*-retinal in

[†] Department of Biochemistry & Molecular Biophysics, University of Arizona.
[‡] Department of Chemistry, University of Arizona.
[§] Department of Physics, University of Arizona.
[||] Department of Chemistry, Columbia University.
[⊥] Current address: Faculté de Pharmacie, Université René Descartes, Paris 75270, France.
[#] Current address: Department of Chemistry, Osaka University, Osaka 560-0043, Japan.
[¶] Current address: Publications Division, American Chemical Society, Washington, DC 20036.

(1) (a) Bockaert, J.; Pin, J. P. *EMBO J.* **1999**, *18*, 1723−1729. (b) Pierce, K. L.; Premont, R. T.; Lefkowitz, R. J. *Nat. Rev. Mol. Cell Biol.* **2002**, *3*, 639−650.
(2) (a) Provencio, I.; Cooper, H. M.; Foster, R. G. *J. Comp. Neurol.* **1998**, *395*, 417−439. (b) Hattar, S.; Liao, H.-W.; Takao, M.; Berson, D. M.; Yau, K.-W. *Science* **2002**, *295*, 1065−1070. (c) Arendt, D.; Tessmar-Raible, K.; Snyman H.; Dorresteijn, A. W.; Wittbrodt, J. *Science* **2004**, *306*, 869−871.
(3) (a) Palczewski, K.; Kumasaka, T.; Hori, T.; Behnke, C. A.; Motoshima, H.; Fox, B. A.; Le Trong, I.; Teller, D. C.; Okada, T.; Stenkamp, R. E.; Yamamoto, M.; Miyano, M. *Science* **2000**, *289*, 739−745. (b) Teller, D. C.; Okada, T.; Behnke, C. A.; Palczewski, K.; Stenkamp, R. E. *Biochemistry* **2001**, *40*, 7761−7772. (c) Okada, T.; Fujiyoshi, Y.; Silow, M.; Navarro, J.; Landau, E. M.; Shichida, Y. *Proc. Natl. Acad. Sci. U.S.A.* **2002**, *99*, 5982−5987. (d) Okada, T.; Sugihara, M.; Bondar, A. N.; Elstner, M.; Entel, P.; Buss, V. *J. Mol. Biol.* **2004**, *342*, 571−583. (e) Li, J.; Edwards, P. C.; Burghammer, M.; Villa, C.; Schertler, G. F. X. *J. Mol. Biol.* **2004**, *343*, 1409−1438.
(4) (a) Sakmar, T. P.; Menon, S. T.; Marin, E. P.; Awad, E. S. *Annu. Rev. Biophys. Biomol. Struct.* **2002**, *31*, 443−484. (b) Hubbell, W. L.; Altenbach, C.; Hubbell, C. M.; Khorana, H. G. *Adv. Protein Chem.* **2003**, *63*, 243−290.
(5) Jäger, S.; Lewis, J. W.; Zvyaga, T. A.; Szundi, I.; Sakmar, T. P.; Kliger, D. S. *Proc. Natl. Acad. Sci. U.S.A.* **1997**, *94*, 8557−8562.
(6) Salgado, G. F. J.; Struts, A. V.; Tanaka, K.; Fujioka, N.; Nakanishi, K.; Brown, M. F. *Biochemistry* **2004**, *43*, 12819−12828.
(7) (a) Pan, D.; Mathies, R. A. *Biochemistry* **2001**, *40*, 7929−7936. (b) Pan, D.; Ganim, Z.; Kim, J. E.; Verhoeven, M. A.; Lugtenburg, J.; Mathies, R. A. *J. Am. Chem. Soc.* **2002**, *124*, 4857−4864. (c) Kukura, P.; McCamant, D. W.; Yoon, S.; Wandschneider, D. B.; Mathies, R. A. *Science* **2005**, *310*, 1006−1009.
(8) (a) Wang, Q.; Schoenlein, R. W.; Peteanu, L. A.; Mathies, R. A.; Shank, C. V. *Science* **1994**, *266*, 422−424. (b) Kochendoerfer, G. G.; Verdegem, P. J. E.; van der Hoef, I.; Lugtenburg, J.; Mathies, R. A. *Biochemistry* **1996**, *35*, 16230−16240.
(9) (a) Brown, M. F.; Chan, S. I. In *Encyclopedia of Nuclear Magnetic Resonance*; Grant, D. M., Harris, R. K., Eds.; Wiley: New York, 1996; pp 871−885. (b) Brown, M. F.; Lope-Piedrafita, S.; Martinez, G. V.; Petrache, H. I. In *Modern Magnetic Resonance*; Webb, G. A., Ed.; Springer: New York, 2006, in press.

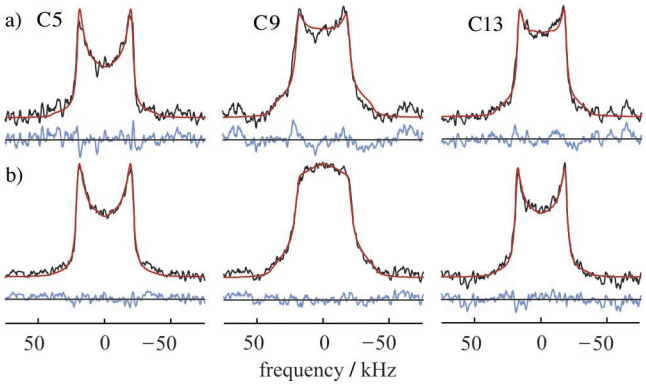

Figure 1. Solid-state ^{2}H NMR spectra for aligned (a) MI/POPC and (b) Rho/POPC (1:50) membranes in MES buffer at pH 7. Data were acquired at −100 °C for MI and −150 °C for the dark state at zero tilt ($\theta = 0°$) for C5, C9, and C13 ^{2}H-labeled methyl groups. Experimental spectra (black) are shown with theoretical simulations (red) and residuals (blue).

metarhodopsin I (MI),[10] which is the precursor to the activated MII state. Our data indicate that the retinylidene moiety is conformationally relaxed adjacent to the C12−C13 bond but not the β-ionone ring in MI. ^{2}H NMR provides a new avenue for investigating conformational changes of the highly strained chromophore of Rho in the course of photoreceptor activation.

Results

In this work, synthetic retinals specifically ^{2}H-labeled at the C5, C9, or C13 methyls were used to regenerate Rho with a single C^2H_3 group per receptor. Membranes comprising Rho and 1-palmitoyl-2-oleoyl-*sn*-glycero-3-phosphocholine (POPC) (1:50) were prepared by detergent dialysis, and were aligned on glass slides[6] by isopotential ultracentrifugation. Rhodopsin was bleached and cryotrapped in the MI state. Solid-state ^{2}H NMR spectroscopy allowed us to establish the orientation of the ^{2}H quadrupolar coupling tensor relative to the membrane frame. Aligned MI/POPC samples and unbleached Rho/POPC membranes[6] were investigated to determine the bond orientation θ_B for the retinylidene C5, C9, or C13 methyl groups.

Representative ^{2}H NMR spectra are shown in Figure 1 for aligned MI/POPC and Rho/POPC membranes below the lipid order−disorder transition (−4 °C). ^{2}H NMR spectra were obtained for single C^2H_3 groups in the case of a membrane protein of molar mass 40 kDa. A closed-form mathematical solution for a semirandom distribution was used to simulate the experimental line shapes. Theoretical ^{2}H NMR spectra were calculated for the oriented samples by assuming a static uniaxial distribution about the membrane normal.[11] The theoretical line shapes depend on both the methyl bond orientation θ_B and the alignment disorder (mosaic spread), which was assumed to be Gaussian with a standard deviation of σ. Superposed on each experimental spectrum is the theoretical spectrum for a static uniaxial distribution of rotating methyl groups. Spectral simulations[11] included the sample tilt θ, the (residual) quadrupolar coupling constant $\langle\chi_Q\rangle$, the intrinsic line width, the standard deviation of the alignment σ, and the methyl bond orientation θ_B. Calculated MI spectra also took into account the presence of about 10% rhodopsin due to incomplete photoconversion.

For the MI state (Figure 1a) compared to the dark state (Figure 1b), the ^{2}H NMR spectra showed a substantial difference for the C9 methyl, with smaller differences for the C5 C^2H_3 and C13 C^2H_3 groups. Calculated ^{2}H NMR line shapes were very sensitive to the bond orientation, and accurately reproduced the angular anisotropy. The retinylidene methyl groups were found to undergo rapid 3-fold rotation within the Rho binding pocket on the ^{2}H NMR time scale ($\approx 10^{-6}$ s), even at −100 °C and below. Off-axial motions were minimal; i.e., the order parameter of the 3-fold axis was $S_{C3} \approx 0.9$ as shown by the residual quadrupolar coupling constant $\langle\chi_Q\rangle = 48-53$ kHz. Apart from the methyl rotation and associated torsional fluctuations, the retinal ligand is held firmly within the rhodopsin binding pocket.

Aligned samples[6] were then subjected to a tilt series vs the magnetic field $\mathbf{B}_0$ to increase the precision of the calculated bond orientation θ_B for the retinylidene C5, C9, or C13 methyl groups. Figure 2 displays the results of global fitting of the spectra as a function of bond orientation θ_B and alignment disorder σ. Generally, the MI samples had a larger mosaic spread of $\sigma = 22-25°$ vs the dark state (18−21°). The different line shape for the C9 methyl of MI vs the dark state is largely due to an increase in σ rather than the bond orientation θ_B, evincing the importance of properly treating the alignment disorder.[11] The root-mean-square-deviation (RMSD) error surfaces showed unambiguous solutions for all three methyl positions, with the possible exception of the C5 methyl of the β-ionone ring, whose minima were not as well-defined. A similar pattern was found for the C5 methyl in the dark state, but with a more pronounced minimum.[6] The nonsymmetric error surface for the C5 methyl may imply that different conformers may be present. For example, significant mobility of the β-ionone ring could give multiple conformations, which would affect the ^{2}H NMR angles and requires further investigation. Upon photoisomerization, the most significant change in θ_B involved the C13 methyl proximal to the retinylidene Schiff base (Table 1).

Discussion

The conformation of 11-*cis*-retinal within the binding pocket of rhodopsin is specified by its isomeric state assuming ideal orbital hybridization. In terms of ideal geometry, the orientation of retinal with respect to the membrane normal is defined by two angular degrees of freedom (Euler angles). However, distortion of the conjugated 11-*cis*-retinal polyene is known to occur due to stereochemical interactions within the rhodopsin binding pocket in conjunction with nonbonded repulsive interactions involving the methyl groups. Various biophysical[5−7] and bioorganic[12] studies indicate that conformational distortion of the retinylidene chromophore of rhodopsin is present in the vicinity of the C6−C7 bond and the C12−C13 bond. Significant deviation of the conjugated 11-*cis*-retinal polyene from ideal hybrid orbital geometry is also evident in the present work. This conformational distortion is related to the storage of light energy and mechanism of activation of rhodopsin in the visual process.[13]

Figure 3 provides an heuristic illustration of how the ^{2}H NMR structure of retinal is calculated in the MI state of photolyzed

(10) Ruprecht, J. J.; Mielke, T.; Vogel, R.; Villa, C.; Schertler, G. F. X. *EMBO J.* **2004**, *23*, 3609−3620.
(11) Nevzorov, A. A.; Moltke, S.; Heyn, M. P.; Brown, M. F. *J. Am. Chem. Soc.* **1999**, *121*, 7636−7643.
(12) (a) Fujimoto, Y.; Ishihara, J.; Maki, S.; Fujioka, N.; Wang, T.; Furuta, T.; Fishkin, N.; Borhan, B.; Berova, N.; Nakanishi, K. *Chem. Eur. J.* **2001**, *7*, 4198−4204. (b) Fujimoto, Y.; Fishkin, N.; Pescitelli, G.; Decatur, J.; Berova, N.; Nakanishi, K. *J. Am. Chem. Soc.* **2002**, *124*, 7294−7302.
(13) (a) Cooper, A. *Nature (London)* **1979**, *282*, 531−533. (b) Gascon, J. A.; Batista, V. S. *Biophys. J.* **2004**, *87*, 2931−2941.

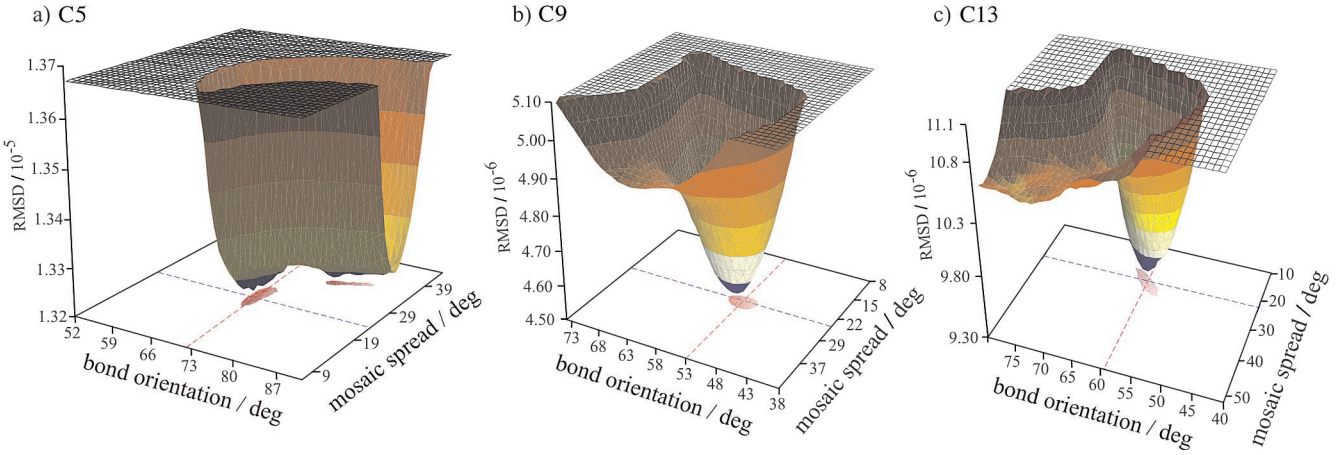

Figure 2. Error surfaces for MI state calculated from RMSD analysis of simulated vs experimental ^{2}H NMR spectra for (a) C5, (b) C9, and (c) C13 methyl groups. Methyl bond orientation θ_B and mosaic spread (σ) are free parameters and range from 0° to 90°. Floors of the three surfaces indicate the minima in the RMSD corresponding to the best fit values of θ_B and σ.

Table 1. Retinal Conformation in Metarhodopsin I State

	bond orientation (θ_B/deg)			torsional angle/deg	
	C5	C9	C13	C5═C6−C7═C8	C11═C12−C13═C14
MI	72 ± 4	53 ± 3	59 ± 3	±32, ±57	±173
dark[a]	70 ± 3	52 ± 3	68 ± 3	−65	+150

[a] From ref 5.

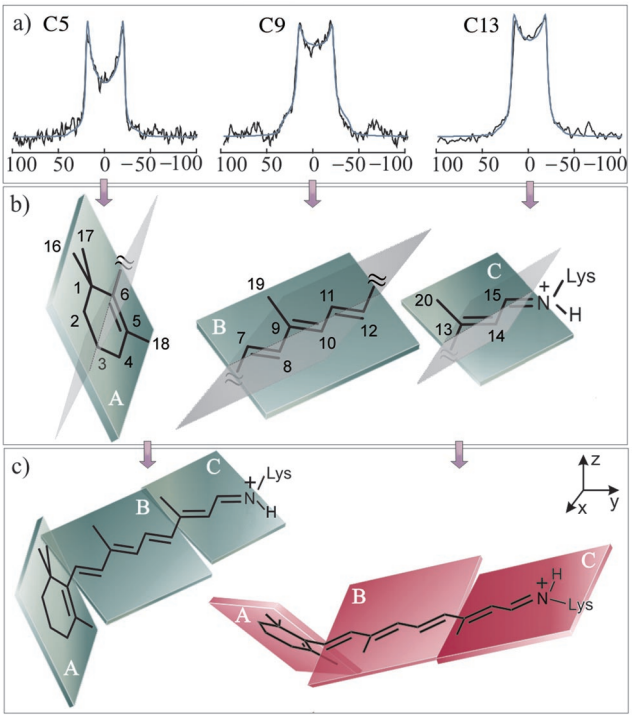

Figure 3. Schematic representation of retinal structure calculations with arrows showing logical flow. (a) Theoretical simulations of ^{2}H NMR spectra provide bond orientations vs membrane normal. (b) Bond vectors together with electronic transition dipole moment define orientations of molecular fragments; two representative orientations are shown for each plane. The atom numbering of retinal follows standard crystallographic nomenclature. (c) Irreducible structures for retinylidene ligand with Schiff base linkage to Lys^{296} of rhodopsin.

rhodopsin. Although many degrees of freedom are present, the retinal conformation in the dark and MI states can be approximated by three planes (here designated as A, B, and C), comprising the polyene chain to either side of the *s-trans* C12−C13 bond, as well as the β-ionone ring (Figure 3).[12] Twisting of the retinal within the individual planes is assumed to be negligible. In this way, the angular degrees of freedom are reduced to knowing the orientations of the parts of the retinal molecule that effectively define the C5═C6−C7═C8 and C11═C12−C13═C14 torsional angles. The applicability of such a three-plane model is supported by recent molecular dynamics simulations[14] and the X-ray crystal structure.[3]

Now, as shown previously for the dark state,[6] each plane is defined by two vectors, and adjacent planes have shared bonds, so that four vectors are needed to describe the structure and orientation of retinal. Such a reduction in the degrees of freedom of the conjugated polyene allows the conformational analysis to be carried out using a relatively small number of angular restraints from the ^{2}H NMR data. The orientations of the planes relative to the membrane normal are given by the angles of the C5, C9, and C13 methyl axes, obtained from fitting the ^{2}H NMR spectra (Figure 3a). Since data for the pro-*R*- and pro-*S*-methyl groups at C1 of the β-ionone ring are lacking, as a fourth angular restraint we use the transition dipole moment obtained from linear dichroism studies,[15] which has a fixed orientation with respect to the retinal axis.[5,16]

The torsion angle $\chi_{i,k}$ between the consecutive planes is calculated as described (cf. Supporting Information).[6] However, this calculation is subject to symmetry-related restrictions as briefly described below. Both the nuclear spin interactions in solid-state ^{2}H NMR[9] and the transition dipole moment[5,15,16] correspond to the Legendre function $P_2(\cos\theta) = (1/2)(3\cos^2\theta - 1)$. They transform according to the totally symmetric representation of the point group $D_{\infty h}$, meaning that the experimental observables are invariant to symmetry operations of inversion, rotation, or reflection, as given by character tables that are found in texts on group theory.[17] For example, the orientation of the methyl axes with respect to the laboratory or membrane frame can point either up or down, so they cannot be distinguished from their supplements. Likewise, rotation about the membrane normal cannot be distinguished, nor can

(14) Lau, P.-W., Pitman, M. C.; Feller, S. E.; Brown, M. F. *Biophys. J.* **2006**, *90*, 442a.
(15) Chabre, M.; Breton, J. *Vision Res.* **1979**, *19*, 1005−1018.
(16) Lewis, J. W.; Einterz, C. M.; Hug, S. J.; Kliger, D. S. *Biophys. J.* **1989**, *56*, 1101−1111.
(17) Cotton, F. A. *Chemical Applications of Group Theory*, 3rd ed.; Wiley: New York, 1990.

reflection across the horizontal membrane plane; there are other symmetry operations as well.[17] The same observations apply to optical measurements of the electronic transition dipole moment.

Concerning each of the four possible orientations of a given plane of the retinal ligand, the adjacent plane has four relative orientations, giving a total of 16 solutions for each dihedral angle (Figure 3b). Most of these can be eliminated by taking into consideration the additional restraints provided by the molecular geometry and solid-state ^{13}C NMR rotational resonance data.[18] For instance, on the basis of ^{2}H NMR data either a twisted 6-*s*-*cis* or a 6-*s*-*trans* conformation of the β-ionone ring is possible.[6] The 6-*s*-*trans* conformer can be excluded by introducing the C8-to-C18 and C8-to-C16/C17 distances between the β-ionone ring and the polyene chain as obtained from the dipolar couplings in solid-state ^{13}C NMR,[18] giving the results in Table 1. (Trapping conditions for MI or inaccuracy in the calculated distance could alter this conclusion; e.g., mobility of the β-ionone ring in MI would favor the shorter C8-to-C18 distance in the 6-*s*-*cis* vs the 6-*s*-*trans* conformer.) Irreducible structures for retinal bound to MI are depicted in Figure 3c, from which the additional solutions are generated by appropriate symmetry operations as described above. The electron density map of MI indicates that the β-ionone ring is strongly localized and its position is similar to the dark state.[10] Hence, in Figure 3c the left conformer is the most likely physical solution, with the N-terminus of Rho at the top. Torsional twisting about the C12−C13 bond[5−7,12] is selectively relaxed in the 11-*trans* isomer of retinal in MI, in agreement with resonance Raman[7] and ^{13}C rotational resonance NMR[18] studies.

Knowledge of the orientation and conformation of retinal within the MI binding pocket is significant for energy storage in vision through photoisomerization of the retinal chromophore and accompanying molecular rearrangements.[4,13,19,20] Our study gives precise data for comparison to quantum mechanical and classical molecular dynamics simulations of receptor activation. Extension of the approach to other GPCRs can stimulate ligand-based drug discovery and the design of new pharmaceutical agents.

Experimental Section

Synthesis of Selectively Deuterated 11-*Z*-Retinals. Isotopically labeled retinals were prepared by total synthesis and were specifically labeled with deuterium at the C5, C9, or C13 methyl groups. Selectively deuterated 11-*Z*-[5-C^2H_3]-retinal, 11-*Z*-[9-C^2H_3]-retinal, and 11-*Z*-[13-C^2H_3]-retinal were obtained via a route analogous to the synthesis of unlabeled retinal.[21] For 11-*Z*-retinal deuterated at the C5, C9, or C13 methyl groups, the aldehyde−tricarbonyliron complex of the precursor was prepared and used for synthesis of the disubstituted *Z*-olefin. The synthesis involved the Peterson reaction using ethyl trimethylsilyl acetate, followed by coupling with diisopropyl cyanomethylphosphonate employing the Horner−Emmons reaction and sodium hydride as the base, decomplexation with $CuCl_2$, and finally DIBAL reduction. The various synthetic retinals were characterized by their UV−visible spectra, their Fourier transform infrared spectra, and their ^{1}H, ^{2}H, and ^{13}C NMR spectra in benzene solution. Deuterium content was established by mass spectrometry in acetone/acetonitrile using positive electrospray ionization (ESI). The (quasi)molecular MH^+ ions were at $m/z = 288.1$, consistent with a single deuterated methyl group, as compared with authentic 11-*Z*-retinal with MH^+ at $m/z = 285.1$. Deuterated 11-*Z*-retinals were stored in the dark as 0.5 mg aliquots in benzene at −70 °C until used.[21]

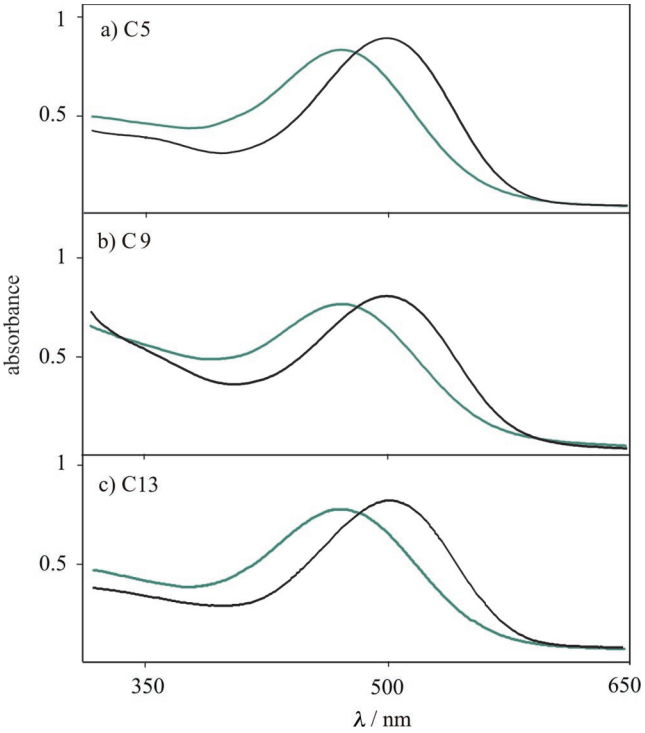

Figure 4. Representative UV−visible spectra of oriented membrane samples used for ^{2}H NMR spectroscopy. Aligned samples are shown containing rhodopsin/POPC (1:50) regenerated with 11-*cis*-retinal labeled at the (a) C5, (b) C9, and (c) C13 methyl groups. Spectra are displayed for aligned membranes containing rhodopsin in the dark state in MES buffer at pH 7 (black) and for the MI photointermediate in MES buffer at pH 7 (blue) formed by irradiation for ≈1.5 min with $\lambda > 550$ nm at 2 °C (order of decreasing λ_{max}). The MI spectra have a characteristic band at $\lambda_{max} \approx 479$ nm.

Preparation of Aligned Membrane Samples containing Metarhodopsin I. Rhodopsin/POPC recombinant membranes (1:50 molar ratio) were prepared in MES buffer, pH range 6.5−7, and oriented on ultrathin glass plates (6 × 12 mm; Marienfeld Glassware, Bad Mergentheim, Germany) by isopotential ultracentrifugation as described.[6] Immediately thereafter, the samples were placed in a glovebox at 2 °C and kept under a gentle stream of argon, until 24−30 glass plates were collected, each containing about 0.9 mg of rhodopsin. The argon gas stream protected the lipids against oxidation while inducing a slow dehydration of the deposited proteolipid film. About 24 plates were hydrated by isopiestic transfer inside a glass chamber containing saturated K_2CO_3 (relative humidity ≈ 43% at 2 °C) for a period of 4−12 h. Metarhodopsin I was prepared by illuminating each of the individual glass plates for 1−2 min at 2 °C with green light (high-pass filter with average transmittance $T > 90\%$ over range 550−700 nm) from a 150-W tungsten−halogen light source (FOSTEC; Auburn, NY), using a fiber optic light guide. Each of the four to five centrifugation runs enabled the preparation of six glass slides; one of the six was always randomly selected for UV−visible spectroscopy to quantify the presence of MI and check for any residual, unbleached rhodopsin. UV−visible spectra were recorded at 1 °C as shown in Figure 4 using

(18) (a) Verdegem, P. J. E.; Bovee-Geurts, P. H. M.; de Grip, W. J.; Lugtenburg, J.; de Groot, H. J. M. *Biochemistry* **1999**, *38*, 11316−11324. (b) Spooner, P. J. R.; Sharples, J. M.; Verhoeven, M. A.; Lugtenberg, J.; Glaubitz, C.; Watts, A. *Biochemistry* **2002**, *41*, 7549−7555. (c) Spooner, P. J. R.; Sharples, J. M.; Goodall, S. C.; Seedorf, H.; Verhoeven, M. A.; Lugtenburg, J.; Bovee-Geurts, P. H. M.; DeGrip, W. J.; Watts, A. *Biochemistry* **2003**, *42*, 13371−13378.
(19) Borhan, B.; Souto, M. L.; Imai, H.; Shichida, Y.; Nakanishi, K. *Science* **2000**, *288*, 2209−2212.
(20) Patel, A. B.; Crocker, E.; Eilers, M.; Hirshfeld, A.; Sheves, M.; Smith, S. O. *Proc. Natl. Acad. Sci. U.S.A.* **2004**, *101*, 10048−10053.
(21) Borhan, B.; Souto, M. L.; Um, J. M.; Zhou, B.; Nakanishi, K. *Chem. Eur. J.* **1999**, *5*, 1172−1175.

a locally constructed glass cryostat with quartz windows. The photolyzed samples gave a characteristic band at $\lambda_{max} \approx 479$ nm which is indicative of MI.[10] In preliminary studies, a small bump in the UV−visible spectra was seen near 500 nm due to nonbleached rhodopsin. After refinement of the conditions for MI the bump at 500 nm was absent. The presence of any residual, nonbleached rhodopsin was manifested by a slight increase in the negative slope of the UV−visible spectra in the region between 500 and 600 nm. We estimated that the amount of unbleached rhodopsin varied from 3 to 8% for the different glass slides, and was <5% for the entire stack used for the ^{2}H NMR experiments. As a final step, ≈24 glass plates were stacked and inserted into a cutoff 8 × 22 mm NMR tube (chilled to −70 °C just before stacking the glass plates) and sealed with a Teflon plug. The glass plates containing the illuminated rhodopsin films were maintained at −70 °C in a freezer and never allowed to warm above −20 °C. The MI/POPC membrane samples used for ^{2}H NMR spectroscopy typically contained 22−25 mg of rhodopsin.

Solid-State ^{2}H NMR Spectroscopy. The solid-state ^{2}H NMR spectra were acquired at 76.77 MHz, using a Bruker AMX-500 spectrometer equipped with a narrow-bore magnet (11.7 T). A home-built, high-power ^{2}H NMR probe was utilized, which was optimized for samples having very weak signals. The ^{2}H NMR probe had an 8-mm diameter × 12-mm long transverse solenoidal radio frequency coil with high-voltage capacitors, and gave a 4.2 μs 90° pulse at 76.77 MHz. The Bruker radio frequency amplifier was used to drive an external boost amplifier (Henry Radio, Los Angles, CA) to increase the power of the transmitter pulses to 600 W. A quadrupolar echo sequence with composite pulses ($135^\circ_{-x}90^\circ_{x}45^\circ_{-x}-\tau-135^\circ_{y}90^\circ_{-y}45^\circ_{y}-\tau$-acquisition) was employed, and was appropriately phase-cycled to acquire the ^{2}H NMR signals. The delay time τ varied from 40 to 70 μs depending on the sample temperature, to avoid acoustical ringing of the radio frequency coil, and the repetition time was typically 0.1−1.5 s depending on the T_{1Z} relaxation time. A total of 16K data points with a dwell time of 0.1 μs was acquired (spectral width using quadrature phase detection of 5 MHz). The quadrupolar echo signals were typically acquired in blocks of 300 000 scans, which were then added and Fourier transformed to give the experimental ^{2}H NMR spectrum. Care was taken to initiate the Fourier transformation at the top of the quadrupolar echo, using locally written data processing software (MATLAB; The MathWorks, Inc., Natick, MA). To avoid spectral distortions due to frequency-dependent phase shifts, no first-order phase correction was applied to any of the spectra. Both quadrature channels were employed for Fourier transformation, and the spectra were not symmetrized, which can lead to artifacts such as virtual quadrupolar splittings.[22] Typically the echo signals were multiplied by a decaying exponential corresponding to a line broadening of 500 Hz in the frequency domain to apodize the spectra. Each ^{2}H NMR spectrum required ≈(0.2−1) × 10^6 scans (≈1−14 days of signal averaging).

Acknowledgment. This work was supported by NIH Grants GM36564 (K.N.) and EY012049 (M.F.B.), and by NASA (M.F.B.). We thank Rosalie Crouch for authentic 11-*Z*-retinal, Constantin Job for electronics assistance, and Wayne Hubbell, Oliver Monti, and Andrei Sanov for helpful discussions.

Supporting Information Available: ^{2}H NMR spectral line shape simulation; analysis of retinal conformation bound to rhodopsin. This material is available free of charge via the Internet at http://pubs.acs.org.

JA058738+

(22) Siminovitch, D. J.; Rance, M.; Jeffrey, K. R.; Brown, M. F. *J. Magn. Reson.* **1984**, *58*, 62−75.